DNA-PKcs PARylation regulates DNA-PK kinase activity in the DNA damage response

YANG HAN[1,2*], FENG JIN[2*], YING XIE[2], YIKE LIU[2,3], SAI HU[1,2], XIAO-DAN LIU[2], HUA GUAN[2], YONGQING GU[2], TENG MA[2,4] and PING-KUN ZHOU[2,3]

[1]Institute for Environmental Medicine and Radiation Hygiene, School of Public Health, University of South China, Hengyang, Hunan 421001; [2]Department of Radiation Biology, Beijing Key Laboratory for Radiobiology, Beijing Institute of Radiation Medicine, Beijing 100850; [3]Institute for Chemical Carcinogenesis, State Key Laboratory of Respiratory Disease, Guangzhou Medical University, Guangzhou, Guangdong 511436; [4]Department of Cellular and Molecular Biology, Beijing Chest Hospital, Capital Medical University/Beijing Tuberculosis and Thoracic Tumor Research Institute, Beijing 101149, P.R. China

Received January 30, 2019; Accepted July 5, 2019

DOI: 10.3892/mmr.2019.10640

Abstract. DNA-dependent protein kinase catalytic subunit (-PKcs) is the core protein involved in the non-homologous end-joining repair of double-strand breaks. In addition, it can form a complex with poly(ADP-ribose) polymerase 1 (PARP1), which catalyzes protein PARylation. However, it is unclear how DNA-PKcs interacts with PARP1 in the DNA damage response and how PARylation affects DNA-PK kinase activity. Using immunoprecipitation, immunofluorescence and flow cytometry the present study found that DNA-PKcs was PARylated after DNA damage, and the PARP1/2 inhibitor olaparib completely abolished DNA-PKcs PARylation. Olaparib treatment prevented DNA-PKcs protein detachment from chromatin after DNA damage and maintained DNA-PK activation, as evidenced by DNA-PKcs Ser2056 phosphorylation. Furthermore, olaparib treatment synergized with DNA-PK inhibition to suppress cell survival. All of the above results are suggestive of the important role of DNA-PKcs PARylation in regulating DNA-PK activity.

Correspondence to: Dr Teng Ma, Department of Cellular and Molecular Biology, Beijing Chest Hospital, Capital Medical University/Beijing Tuberculosis and Thoracic Tumor Research Institute, 2 Research Building, 97 Machang, Tongzhou, Beijing 101149, P.R. China
E-mail: mateng82913@163.com

Dr Ping-Kun Zhou, Department of Radiation Biology, Beijing Key Laboratory for Radiobiology, Beijing Institute of Radiation Medicine, 27 Taiping Road, Haidian, Beijing 100850, P.R. China
E-mail: zhoupk@bmi.ac.cn

*Contributed equally

Key words: parylation, double strand break repair, non-homologous end joining repair, autophosphorylation

Introduction

DNA double-strand breaks (DSBs) are the most harmful type of DNA lesions and can affect various processes including cell cycle progression, genomic stability and the induction of tumorigenesis. There are two distinct mechanisms of DNA DSB repair: Homologous recombination (HR) and non-homologous end-joining (NHEJ) (1). Three major DNA damage-activated PI3K-related serine/threonine protein kinases, DNA-protein kinase (-PK), ataxia-telangiectasia mutated (ATM), and ATR serine/threonine kinase (ATR) (2), participate in repair pathways. The DNA-dependent protein kinase catalytic subunit (DNA-PKcs) plays an important role during the repair of DNA DSBs. The autophosphorylation of DNA-PKcs represents the activation of DNA-PK and regulates its own dynamics at DNA DSBs (3).

Posttranslational modifications of proteins such as ubiquitination, neddylation, acetylation and polyADP-ribosylation are significant mechanisms that regulate many cellular processes. PARylation plays crucial roles in DNA repair, replication, transcription and cell death (4-6). The poly(ADP-ribosylation) reaction, in which DNA-dependent poly(ADP-ribose) (PAR) is synthesized from nicotinamide mononucleotide (NAD) by poly(ADP-ribose) polymerases (PARPs) and poly(ADP-ribose) glycohydrolase (PARG), regulates the hydrolysis of PAR and was discovered in 1963 (7,8). After cells are exposed to ionizing radiation, free radicals and alkylating agents, PARP1 binds rapidly to DNA DSB sites, resulting in PAR modification. This process uses NAD^+ as a substrate and leads to the formation of poly(ADP-ribose) polymers on target proteins, and intracellular NAD^+ is depleted in this process. However, poly(ADP-ribose) has a short half-life *in vivo* since it is rapidly degraded by PARG (2-5 min after polymer formation) (9). The PARP family has 16 members, but only PARP1 and PARP2 are closely associated with DSBs (10). Furthermore, PARP1, a 116 kDa protein, contains a DNA binding domain, a central auto-modification domain and a C-terminal catalytic domain (11,12) and has 18 distinct isoforms in humans (13).

PARP1 is more important than PARP2 in DSB repair as PARP1 affects several key HR factors, including BRCA1, exonuclease 1 and BRCA2, and acts as a stress sensor and a stress response mediator in biological systems (14). PARP1 has been reported to mediate MRN complex recruitment to DSBs in a γ-histone family member 2AX (H2AX)- and mediator of DNA damage checkpoint protein 1-independent manner (15). PARP1 and MRN together mediate ATM accumulation and the phosphorylation of H2AX, and stabilize the DNA damage response factor at the DNA damage site (16). PARP1 substrates include PARP1 itself, histones, DNA repair proteins, transcription factors and chromatin modulators (17). PARP1 poly-ADP-ribosylates BRCA1, targeting its DNA binding domain and reducing its affinity for DNA (18). DNA-PKcs was previously reported to be modified by IFNγ-induced PARylation (18). However, it is unclear how PARP1 affects DNA-PKcs in the DNA damage response.

The present study identified the PAR modification of DNA-PKcs after DNA damage. The inhibition of PARylation increases the chromatin binding of DNA-PKcs and DNA-PKcs Ser2056 phosphorylation, and the synergistic inhibition of PARylation and DNA-PK activity suppresses cell survival.

Materials and methods

Cell culture and transfection. Hela cells were purchased from American Type Culture Collection. These cells were cultivated at 37˚C in a humidified incubator containing 5% CO_2. The cells were grown in DMEM supplemented with 10% FBS (Gibco; Thermo Fisher Scientific, Inc.), penicillin and streptomycin.

Antibodies and chemicals. The following specific antibodies were used in the present study: PAR (Abcam; cat. no. ab14459), DNA-PKcs (Invitrogen; Thermo Fisher Scientific, Inc.; MA5-13238), mouse IgG (Santa Cruz Biotechnology, Inc.; cat. no. sc-2025), PARP-1 (Santa Cruz Biotechnology, Inc.; cat. no. sc-7150), ATM (Santa Cruz Biotechnology, Inc.; cat. no. sc-23921), Ku70 (Abcam; cat. no. ab3114), Ku80 (Abcam; cat. no. ab119935), DNA-PKcs S2056 (Abcam; cat. no. ab18192), DNA-PKcs T2609 (Abcam; cat. no. ab4194), γ-H2AX (Abcam; cat. no. ab11174), phosphorylated (p)-ATM (Cell Signaling Technology, Inc.; cat. no. 13050S), DAPI (Sigma-Aldrich; Merck KGaA; cat. no. D9542), β-actin (Beijing Zhongshan Golden Bridge Biotechnology Co., Ltd.; cat. no. TA-09), GAPDH (Beijing Zhongshan Golden Bridge Biotechnology Co., Ltd.; cat. no. TA-08), Alexa Flour® 488 goat anti-mouse IgG (H+L; Invitrogen; Thermo Fisher Scientific, Inc.; cat. no. 1915874), and Alexa Flour® 568 goat anti-rabbit IgG (H+L; Invitrogen; Thermo Fisher Scientific, Inc.; cat. no. 1704462), anti-mouse IgG, AP-linked antibody (Cell Signaling Technology, Inc.; cat. No 7056), anti-rabbit IgG, AP-linked antibody (Cell Signaling Technology, Inc.; cat. no. 7054), histone 3.1 (Signalway Antibody LLC.; cat. no. 21137-1). The chemical inhibitor olaparib (cat. no. AZD2281), the PARP1 inhibitor UPF1069 (cat. no. S8038), the PARP1 inhibitor NMS-P118 (cat. no. S8363) and DNA-PK inhibitor NU7441 (cat. no. S2638) were purchased from Selleck Chemicals. DMSO was purchased from InnoChem LLC.

Immunoprecipitation and western blotting. NETN buffer 300 [20 mM Tris-HCL (pH 8.0), 300 mM NaCl, 1 mM EDTA and 0.5% Nonidet P-40] was used to lyse the cells at 4˚C for 10 min. Then NETN buffer 100 [20 mM Tris-HCL (pH 8.0), 100 mM NaCl, 1 mM EDTA and 0.5% Nonidet P-40] was used to lyse the cells at 4˚C for 5 min. After the removal of the cell debris by centrifugation (12,000 x g for 10 min at 4˚C), the supernatant was collected and incubated with IgG (1 μg/ml) and protein A/G (Santa Cruz Biotechnology, Inc.; 20 μl) with rotation for 1 h at 4˚C for preclearing. Then, the precipitate was removed by centrifugation (12,000 x g for 10 min at 4˚C) and the supernatant was collected and incubated with an antibody against DNA-PKcs (1 μg/ml) and protein A/G (Santa Cruz Biotechnology, Inc.; 40 μl) with rotation overnight at 4˚C. After that, the protein A/G was washed three times with NETN 100 buffer and boiled with 5X SDS loading buffer at 100˚C for 10 min. The samples were then subjected to SDS-PAGE and immunoblotting with specific antibodies.

The concentration was measured using a NanoDrop™ 2000C (Thermo Fisher Scientific, Inc.) and 40 μg was loaded per lane on 6% SDS PAG gels. Proteins were transferred to nitrocellulose membranes and blocked with 5% BSA for 1 h at room temperature. Membranes were incubated overnight at 4˚C with the following primary antibodies: DNA-PKcs (1:500) and PAR (1:1,000), GAPDH (1:1,000) and histone 3.1 (1:1,000). After washing, membranes were incubated with secondary antibodies (1:3,000) at room temperature for 1 h. The membranes were washed twice and SuperSignal™ West Pico PLUS Chemiluminescent Substrate (Thermo Fisher Scientific, Inc.) was uniformly added to the membrane. Bands were visualized using an ImageQuant LAS 500 and the ImageQuant LAS 500 1.1.0 software (GE Healthcare Life Sciences).

For chromatin fractionation, HeLa cells were lysed with NETN 100 buffer [20 mM Tris-HCl (pH 8.0), 100 mM NaCl, 1 mM EDTA, and 0.5% Nonidet P-40] for 30 min on ice. The soluble fractions were then collected after centrifugation at 12,000 x g for 10 min at 4˚C, and the pellets were washed twice with PBS and once with ddH_2O. Then, they were treated with 0.2 M HCl to release histones and chromatin-bound proteins, which were then neutralized with 1 M Tris-HCl (pH 8.5). Both fractions were subjected to electrophoresis and western blotting as aforementioned, and probed with antibodies as indicated.

Immunofluorescence. HeLa cells ($8.8x10^6$) were irradiated with the indicated doses of irradiation (IR). After incubation for 0, 1, 2, 4 and 8 h, the cells were fixed in 4% paraformaldehyde at room temperature for 30 min and permeabilized with 0.3% Triton X-100 in 1X PBS for 30 min at room temperature. After blocking nonspecific antibody binding sites with 3% BSA in 1X PBS, the cells were incubated with DNA-PKcs S2056 (1:100) and γ-H2AX (1:100) at room temperature for 60 min. Then, cells were washed with 1X PBS three times and incubated with a secondary antibodies (1:400; Alexa Flour® 488 goat anti-mouse IgG and Alexa Flour® 568 goat anti-rabbit IgG) in the dark at room temperature for 60 min. Then, the slides were washed three times with 1X PBS and the cells were stained for 10 min at room temperature with DAPI to visualize nuclear DNA. Coverslips were placed on glass slides with anti-fade solution, and the results were visualized using a ZEISS fluorescence microscope.

Cell colony formation assay. HeLa cells were seeded in 35 mm dishes at different cell concentrations as indicated and allowed to attach. Then, different concentrations of olaparib (1 and 10 μM) were added, and DMSO was used as a control, for 1 h at 37˚C. After drug treatment, the cells were treated with different irradiation doses (0, 0.5, 1, 2, 4 and 8 Gy). The cells were cultured at 37˚C in a humidified incubator in an atmosphere containing 5% CO_2, and were grown in DMEM supplemented with 10% FBS, penicillin, streptomycin and olaparib. The cells were maintained for 10-14 days. Only colonies containing ≥50 cells were scored.

Cell proliferation assay. HeLa cells in the logarithmic growth phase ($5x10^4$ cells/ml) were prepared as cell suspensions and seeded into 6-well cell culture plates (3 ml/dish; n=3). After the cells had attached, different inhibitors [DMSO, NU7441 (5 μM), olaparib (10 μM), and olaparib (10 μM) + NU7441 (5 μM)] were added to the culture for 1 h at 37˚C, an equal volume of DMSO was used as the control. The number of cells on the 1st, 2nd, 3rd, 4th, 5th and 6th days was determined using flow cytometry. Briefly, cells were collected using 0.25% trypsin and the total number of cells in the cell suspension was directly measured by flow cytometry (NovoCyte; ACEA Biosciences, Inc.) and the NovoExpress 1.3.0 software (ACEA Biosciences, Inc.).

NHEJ assay. Before transfection, a NHEJ-GFP plasmid was digested with HindIII enzyme overnight at 37˚C and recovered using AxyPrep DNA Gel Extraction kit (Axygen; Corning, Inc.), according to the manufacturer's instructions. The cells were transfected with 1 μg of pCherry and 1 μg of the digested NHEJ-GFP plasmid (gifts from Dr Zhenkun Lou; Division of Oncology Research, Mayo Clinic, USA) and mixed with 5 μl of Lipofectamine 2000™ (Invitrogen; Thermo Fisher Scientific, Inc.), as described previously (18). Following 6 h, the culture medium of the transfected cells was replaced with medium containing olaparib (10 μM) or NU7441 (5 μM) and further cultured for 20 h at 37˚C. The cells were trypsinized (0.25%) and resuspended in PBS. The cellular fluorescence was measured by flow cytometry analysis as previously described (19).

HR assay. HeLa cells ($3x10^5$) were pretreated with NU7441 (5 μM) or olaparib (10 μM) for 1 h at 37˚C. Then, they were transfected with a single copy of a DR-GFP, I-*Sce*I expression plasmid and with a pCherry plasmid used as a transfection efficiency control (gifts from Dr Zhenkun Lou; Division of Oncology Research, Mayo Clinic, USA) (19). The cells were harvested 3 days after transfection and subjected to flow cytometry analysis (NovoCyte; ACEA Biosciences, Inc.) and the NovoExpress 1.3.0 software (ACEA Biosciences, Inc.), as previously described (19); the GFP-positive cell population was measured. The mean values were obtained from three independent experiments. Little variation was observed among the three independent experiments. In addition, cell viability was also examined before transfection under a microscope using trypan blue staining for 30 min at room temperature. All of the groups exhibited >90% viability.

Cell synchronization and cell cycle analysis. HeLa cells ($3x10^5$) were incubated with 2 mM thymidine for 17 h at 37˚C, cultured in fresh medium for 10 h, and then treated with thymidine again for a further 13 h. The cells were collected at different times (S phase, 4.5 h; G2/M phase 8 h; G0/G1 phase, 14 h) after release for cell cycle analysis and western blotting, as aforementioned. The cells were washed with prechilled PBS, treated with 100 μg/ml RNase in PBS and stained with 10 μg/ml propidium iodide for 10 min at room temperature. The cell cycle was analyzed using a flow cytometer (NovoCyte; ACEA Biosciences, Inc.) and the NovoExpress 1.3.0 software (ACEA Biosciences, Inc.).

Statistical analysis. Statistical analyses were conducted using SPSS version 23.0 (IBM Corp.). The statistical significance analysis of the experimental data was performed by t-test for two group comparisons or ANOVA followed by Dunnett's post hoc test for multiple group comparison. $P<0.01$ was considered to indicate a statistically significant difference.

Results

DNA-PKcs is modified by PARylation after DNA damage. Since DNA-PKcs interacts with PARP1, it is possible that DNA-PKcs is the substrate of PARP1. To test if DNA-PKcs can be modified by PARylation, the present study examined the DNA-PKcs PARylation status by immunoprecipitation. First, endogenous DNA-PKcs was immunoprecipitated from cells after treatment with different doses of IR. The results revealed that DNA-PKcs PARylation increased as the IR dose increased (Fig. 1A). Next, DNA-PKcs was immunoprecipitated by a PAR antibody IP, and IR treatment increased the amount of DNA-PKcs pulled down (Fig. 1B). These results suggest that DNA-PKcs PARylation is induced by IR. The present study also investigated DNA-PKcs PARylation in different phases of the cell cycle. When the cells were synchronized in the G1, S, and G2 phases, either PAR IP or DNA-PKcs IP was performed. The results indicated that more DNA-PKcs PARylation was seen in the S phase (Fig. S1). Furthermore, when the PARP1/2 inhibitor olaparib was administered to the cells, DNA-PKcs PARylation was reduced at a concentration of 1 μM and abolished at a concentration of 10 μM (Fig. 1C). Since olaparib cannot distinguish between PARP1 and PARP2, the effects of the specific PARP1 inhibitor NMS-P118 and the PARP2 inhibitor UPF1069 on DNA-PKcs PARylation were evaluated. The results revealed that both PARP1 and PARP2 are required for DNA-PKcs PARylation (Fig. S2A), suggesting the redundant roles of PARP1 and PARP2, as previously reported (20).

Next, the present study explored if DNA-PKcs PARylation can affect the DNA-PKcs/Ku70/Ku80 complex. Since the DNA-PKcs/Ku70/Ku80 complex binds DNA ends and is activated by broken DNA ends (21), the chromatin fraction content of the complex after olaparib treatment was examined. The results demonstrated that all three proteins were retained on chromatin (Fig. 1D). These results indicate that overall PARylation inhibition activates the DNA-PK complex and that DNA-PKcs PARylation can suppress DNA-PK activity.

Olaparib treatment increases DNA-PKcs phosphorylation. DNA-PKcs phosphorylation is critical for DNA-PK activity and NHEJ repair (22). To test if the inhibition of DNA-PKcs PARylation by olaparib can affect DNA-PK activity, the present

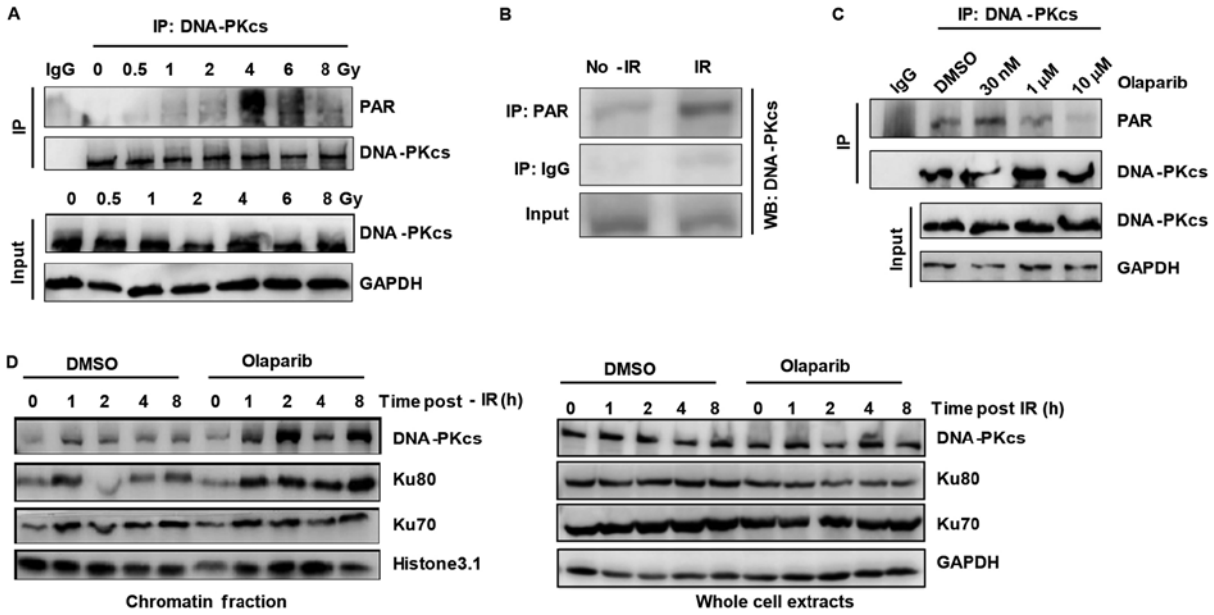

Figure 1. DNA-PK is modified by PAR in response to DNA damage. (A) IP with an anti-DNA-PKcs antibody was performed to detect the PAR modification of DNA-PKcs in HeLa cells after treatment with different irradiation doses (0, 0.5, 1, 2, 4, 6 and 8 Gy). The cells were harvested 2 h after irradiation and then lysed. (B) Western blotting was used to detect DNA-PKcs in the IP product of the anti-PAR antibody from HeLa cells treated with or without irradiation. (C) The effect of olaparib on the PARylation of DNA-PKcs. HeLa cells were treated with different concentrations of olaparib. After 24 h, the cells were harvested and lysed, and IP was used to detected the PAR modification of DNA-PKcs. (D) The effect of olaparib on the chromatin binding of DNA-PKcs in irradiated HeLa cells. DNA-PKcs, DNA-dependent protein kinase catalytic subunit; PAR, poly(ADP-ribose); IP, immunoprecipitation; IR, irradiation.

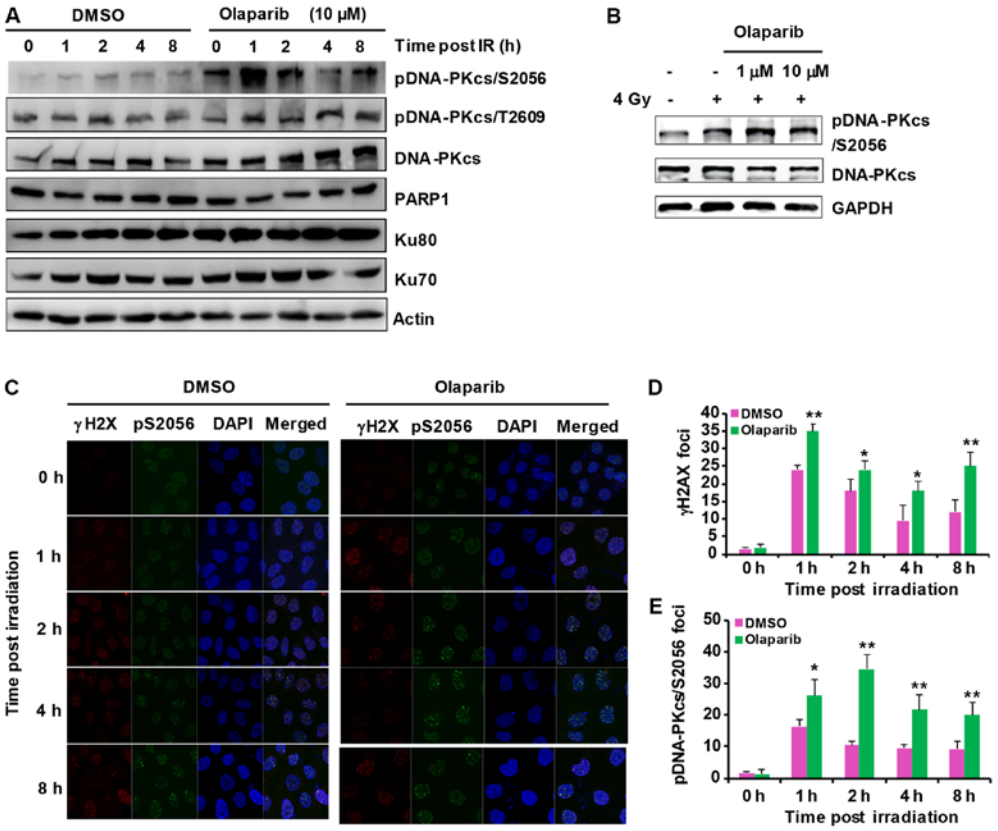

Figure 2. Olaparib treatment promotes the autophosphorylation of DNA-PKcs. (A) The effect of olaparib on the phosphorylation of DNA-PKcs in response to IR. HeLa cells were treated with 10 μM olaparib for 24 h and irradiated with 8 Gy IR. After 1, 2, 4 and 8 h, the expression of phosphorylated DNA-PKcsSer2056 and DNA-PKcsThr2609 was detected by western blotting. (B) HeLa cells were treated with 1 or 10 μM olaparib for 24 h, and the cells were irradiated with 8 Gy IR. After 1 h, the expression of phosphorylated DNA-PKcs/S2056 was detected by western blotting. The effects of olaparib on the formation of γH2AX and DNA-PKcs/S2056 foci were detected by immunofluorescence staining in 8 Gy-irradiated HeLa cells. (C) The dynamic changes in γH2AX foci in 8 Gy-irradiated HeLa cells (magnification x100). (D) The dynamic changes in γH2AX foci in 8 Gy-irradiated HeLa cells. (E) The dynamic changes in DNA-PKcs/S2056 foci in 8 Gy-irradiated HeLa cells. *P<0.05 and **P<0.01 vs. DMSO treatment. DNA-PKcs, DNA-dependent protein kinase catalytic subunit; IR, irradiation; γH2AX, γ-histone family member 2AX; PARP1, poly(ADP-ribose) polymerase 1.

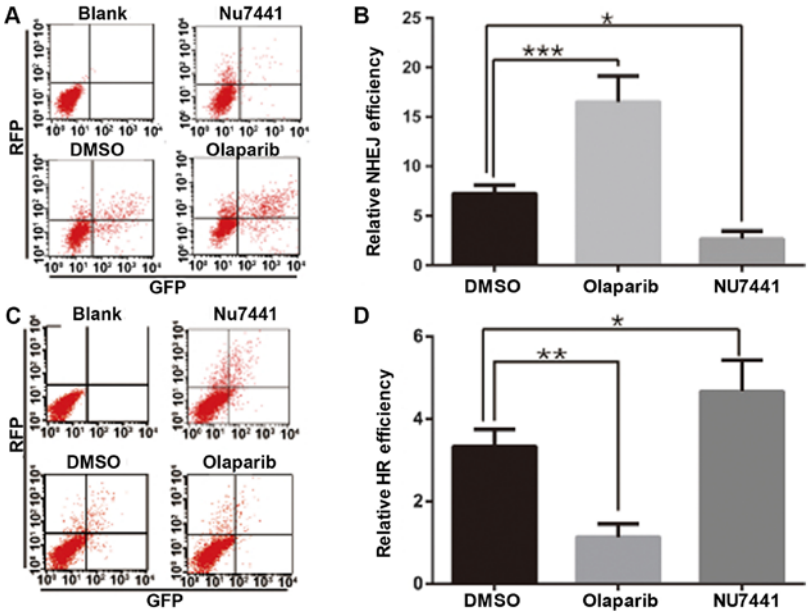

Figure 3. Olaparib treatment activates NHEJ repair. (A and B) HeLa cells were transfected with NHEJ-GFP and a pCherry plasmid for 6 h, the medium was replaced with medium containing 10 μM olaparib or 10 μM NU7441 for 20 h, and then cells were collected. Flow cytometry was used to determine the GFP/RFP double-positive ratio, with the DMSO group as a control. (C and D) HeLa cells were transfected with Dr-GFP, I-SceI and pCherry plasmids for 6 h, the medium was replaced with medium containing 10 μM olaparib or 10 μM NU7441 for 20 h, and then cells were collected. Flow cytometry was used to determine the GFP/RFP double-positive ratio. *P<0.05, **P<0.01, ***P<0.001. NHEJ, non-homologous end-joining; GFP, green florescent protein; RFP, red fluorescent protein; HR, homologous recombination.

study compared DNA-PKcs Ser2056 and Thr 2609 phosphorylation with and without olaparib treatment. The results showed that DNA-PKcs Ser2056 phosphorylation increased while DNA-PKcs Thr 2609 phosphorylation did not change (Fig. 2A and B). These results indicate that olaparib treatment promotes DNA-PK activity through both the inhibition of DNA-PKcs PARylation and the induction of DNA damage. Likewise, treatment with both the PARP1 inhibitor NMS-P118 and the PARP2 inhibitor UPF1069 increased DNA-PKcs Ser2056 phosphorylation (Fig. S2B). Similar results were observed by immunofluorescence staining. DNA-PKcs Ser2056 increased more in the inhibitor-treated groups when compared with the DMSO group and was accompanied by increased γ-H2AX foci (Fig. 2C-E).

Olaparib treatment results in enhanced NHEJ repair. Based on the above findings, one can deduce that PARylation regulates DNA-PKcs Ser2056 phosphorylation. DNA-PKcs Ser2056 phosphorylation is critical for DNA-PK activity and DNA-PKcs conformation (23). Since DNA-PK is the initiator of NHEJ repair, the present study explored NHEJ activity after olaparib treatment. The NHEJ reporter assay indicated that NHEJ repair was significantly boosted after olaparib treatment, while NU7441, as a control, inhibited NHEJ. Furthermore, HR repair was inhibited, suggesting that olaparib treatment can directly induce DNA-PK activation (Fig. 3).

Olaparib increases the radiosensitivity of cells. Sustained DNA-PK activation can hinder the completion of NHEJ and threaten cell survival (24). Therefore, the present study sought to determine if olaparib can increase the radiosensitivity of cells, which was tested by cell colony formation experiments. The results showed that 1 μM olaparib sensitized the cells to different doses of ionizing radiation (Figs. 4A, and S3A and B).

NU7441 is an inhibitor of the kinase activity of DNA-PKcs; thus, the simultaneous inhibition of DNA-PKcs kinase activity and PARylation may have an effect on cell clonogenic formation. The results showed that, when used together, olaparib and NU7441 more significantly reduced cell survival than treatment with olaparib alone (Fig. 4B).

In addition, cell proliferation was also examined after either Olaparib or NU7441 treatment or a combination of both inhibitors. As indicated in Fig. 4C, both Olaparib and NU7441 decreased the cell proliferation rate.

The present study demonstrates a model for DNA-PKcs PARylation and how PARylation affects DNA-PKcs activity (Fig. 5). Both DNA-PKcs kinase activity and PARylation are important regulators of radiosensitivity.

Discussion

DNA-PKcs forms a complex with PARP1 (25), and DNA-PKcs is PARylated by PARP-1 in an IFN-γ- and p53-dependent manner (18). The present study reports that DNA-PKcs is PARylated after DNA damage and that PARylation inhibition causes enhanced DNA-PKcs autophosphorylation and NHEJ repair. Our findings therefore link DNA-PKcs PARylation to DNA damage and substantiates the role of PARP1 in NHEJ repair.

The DNA-PK complex initiates NHEJ by binding broken DNA ends and phosphorylates downstream NHEJ factors (26). According to a previous study, DNA-PKcs T2609 is involved in the DNA damage response and phosphorylated by ATM. However, DNA-PKcs T2609 is not essential for NHEJ repair (27). DNA-PKcs S2056 is critical for the DNA-PKcs function in NHEJ. DNA-PKcs Ser2056 autophosphorylation is critical for DNA-PKcs detachment from DSB sites and the completion of NHEJ (28). Based on the present results, DNA-PKcs PARylation can retain DNA-PKcs on chromatin

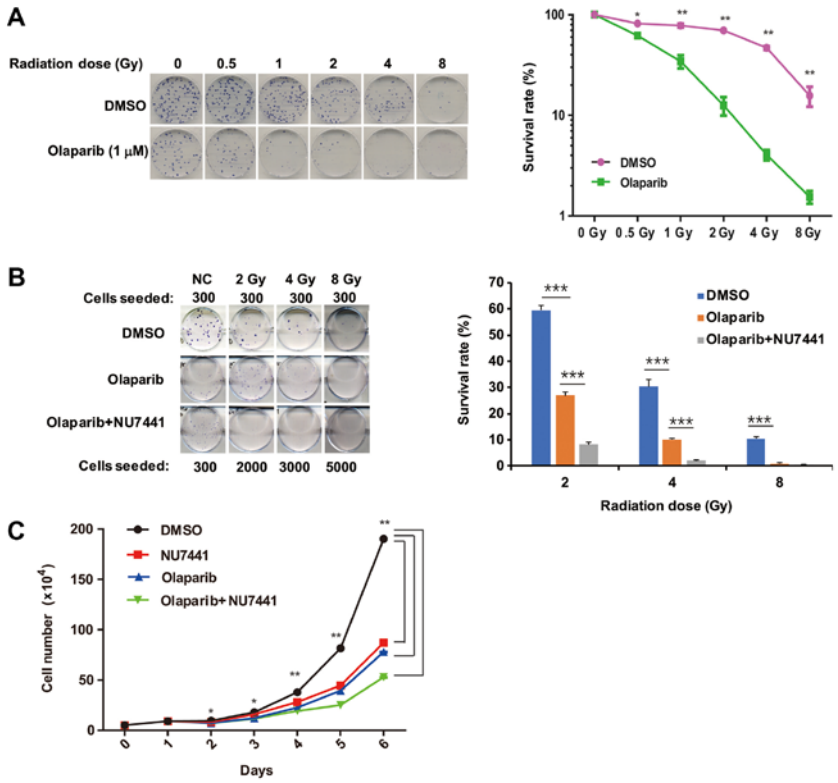

Figure 4. Olaparib treatment sensitizes cells to ionizing radiation. (A) Clonogenic assay. After trypsinization, 300 HeLa cells were plated. Once cells had attached, they were treated with olaparib for 1 h and then irradiated. The DMSO group was used as a control. The cells were cultured for two weeks, and the surviving colonies were observed and counted. *P<0.05 and **P<0.01. (B) The effect of combinational treatment with olaparib and the DNA-PKcs inhibitor NU7441 on the cell colony formation of irradiated HeLa cells. After trypsinization, HeLa cells were seeded at different cell concentrations as indicated (in DMSO controls 300 cells seeded/plate). After the cells were attached, the cells were treated with olaparib (10 μM), or olaparib (10 μM) and NU7441 (5 μM) for 1 h and then irradiated. The DMSO group was used as a control and cultured continuously for two weeks. Colonies containing 50 or more cells were scored. ***P<0.001, as indicated. (C) HeLa cells were prepared as cell suspensions of $5x10^4$ cells/ml and seeded into 6-well cell culture plates (3 ml/dish, n=3). After the cells were attached, different inhibitors [DMSO, NU7441 (5 μM), olaparib (10 μM), and olaparib (10 μM) + NU7441 (5 μM)] were added to the culture. The number of cells was counted by flow cytometry to calculate the mean concentration of each group on each day. *P<0.05 and **P<0.01. DNA-PKcs, DNA-dependent protein kinase catalytic subunit.

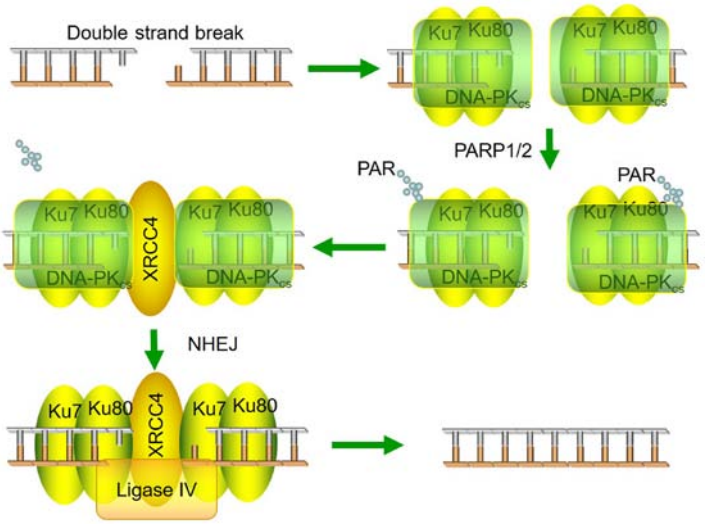

Figure 5. The scheme of DNA-PKcs PARylation in non-homologous end-joining repair. DNA-PKcs, DNA-dependent protein kinase catalytic subunit.

and cause the continuous activation of DNA-PK. The aberrant activation of DNA-PK can block other repair factors from chromatin and hinder the completion of NHEJ repair. On the other hand, olaparib treatment can cause DNA damage since HR is repressed. PARylation is possibly required for DNA-PKcs detachment from chromatin and kinase deactivation. DNA-PK deactivation leads to deficiencies of the NHEJ pathway (28) but may be crucial for successful HR repair.

PARP1 is the major enzyme of the PARP family responsible for PARylation (11,29). It is unknown whether other accessory factors also account for PARylation. The present results also indicated the redundant role of PARP1 in DNA-PKcs PARylation. TrpRS has been reported as one of the 10 class I tRNA synthetases that act as bridging proteins between DNA-PKcs and PARP1 (18). We previously found that tankyrase 1 binding protein 1 (TNKS1BP1) functions in DNA DSB repair by facilitating PARP-1-dependent DNA-PKcs autophosphorylation (30). It would be of interest to determine whether TNKS1BP1 functions as the bridging protein for DNA-PKcs and PARP1 in DNA damage-induced DNA-PKcs PARylation.

DNA-PKcs PARylation can alter kinase activity, but the detailed mechanisms are not understood. Structural analysis is needed to determine the conformational changes after DNA-PKcs PARylation. In a study by Sajish *et al* (18) the DNA-PKcs/Ku70/80/PARP-1 complex, which forms in the presence of damaged DNA, and the DNA-PKcs/TrpRS/PARP-1 complex were mutually exclusive. It is plausible that the DNA-PKcs/Ku70/80/PARP-1 and DNA-PKcs/TNKS1BP1/PARP-1 complexes are mutually exclusive too (18). However, it is notable that TNKS1BP1 promotes DNA-PKcs autophosphorylation while DNA-PKcs PARylation may suppress DNA-PKcs autophosphorylation.

How DNA-PKcs PARylation suppresses its autophosphorylation remains unknown. It is known that serine is the major site for protein PARylation (31). Therefore, it is possible that the conventional DNA-PKcs autophosphorylation sites are also PARylation sites. The interaction between autophosphorylation and PARylation may be an important mechanism of NHEJ repair completion. Olaparib increases the radiation sensitivity of cells through the activation of DNA-PK, thereby providing a possible future treatment for cancer.

In conclusion, DNA-PKcs PARylation is a newly identified player in regulating NHEJ repair. It may answer the question of how NHEJ is completed and how the choice between HR and NHEJ repair is made.

Acknowledgements

Not applicable.

Funding

The present study was supported by grants from the National Key Basic Research Program (973 Program) of MOST, China (grant no. 2015CB910601) and the National Natural Science Foundation of China (grant nos. 81530085, 31570853, 81602799, 31870847).

Availability of data and materials

The datasets used and/or analyzed during the current study are available from the corresponding author on reasonable request.

Authors' contributions

YH and FJ carried out the experiments. TM wrote the manuscript with support from PZ. YX, YL and SH performed cell culture. HG, YG and XL helped with data analysis, data interpretation and supervised the project. TM and PZ conceived the original idea. PZ supervised the project.

Ethics approval and consent to participate

Not applicable.

Patient consent for publication

Not applicable.

Competing interests

The authors declare that they have no competing interests.

References

1. Zhou PK: DNA damage, signaling and repair: Protecting genomic integrity and reducing the risk of human disease. Chin Sci Bull 56: 3119-3121, 2011.
2. Durocher D and Jackson SP: DNA-PK ATM and ATR as sensors of DNA damage variations on a theme? Curr Opin Cell Biol 13: 225–231, 2001.
3. Dobbs TA, Tainer JA and Lees-Miller SP: A structural model for regulation of NHEJ by DNA-PKcs autophosphorylation. DNA Repair (Amst) 9: 1307-1314, 2010.
4. Witze ES, Old WM, Resing KA and Ahn NG: Mapping protein post-translational modifications with mass spectrometry. Nat Methods 4: 798-806, 2007.
5. Brown JS and Jackson SP: Ubiquitylation, neddylation and the DNA damage response. Open Biol 5: 150018, 2015.
6. Oliver FJ, Menissier-de-Murcia J and de Murcia G: Poly(ADP-ribose) polymerase in the cellular response to DNA damage, apoptosis, and disease. Am J Hum Genet 64: 1282–1288, 1999.
7. Chambon P, Weill JD and Mandel P: Nicotinamide mononucleotide activation of new DNA-dependent polyadenylic acid synthesizing nuclear enzyme. Biochem Biophys Res Commun 11: 39-43, 1963.
8. Cohen MS and Chang P: Insights into the biogenesis, function, and regulation of ADP-ribosylation. Nat Chem Biol 14: 236-243, 2018.
9. Slade D, Dunstan MS, Barkauskaite E, Weston R, Lafite P, Dixon N, Ahel M, Leys D and Ahel I: The structure and catalytic mechanism of a poly(ADP-ribose) glycohydrolase. Nature 477: 616-620, 2011.
10. Lüscher B, Bütepage M, Eckei L, Krieg S, Verheugd P and Shilton BH: ADP-Ribosylation, a multifaceted posttranslational modification involved in the control of cell physiology in health and disease. Chem Rev 118: 1092-1136, 2018.
11. Barkauskaite E, Jankevicius G and Ahel I: Structures and mechanisms of enzymes employed in the synthesis and degradation of PARP-dependent protein ADP-ribosylation. Mol Cell 58: 935-946, 2015.
12. Krishnakumar R and Kraus WL: The PARP side of the nucleus: Molecular actions, physiological outcomes, and clinical targets. Mol Cell 39: 8-24, 2010.
13. Gibson BA and Kraus WL: New insights into the molecular and cellular functions of poly(ADP-ribose) and PARPs. Nat Rev Mol Cell Biol 13: 411-424, 2012.
14. Luo X and Kraus WL: On PAR with PARP: Cellular stress signaling through poly(ADP-ribose) and PARP-1. Genes Dev 26: 417-432, 2012.
15. Haince JF, McDonald D, Rodrigue A, Dery U, Masson JY, Hendzel MJ and Poirier GG: PARP1-dependent kinetics of recruitment of MRE11 and NBS1 proteins to multiple DNA damage sites. J Biol Chem 283: 1197-1208, 2008.
16. Haince JF, Kozlov S, Dawson VL, Dawson TM, Hendzel MJ, Lavin MF and Poirier GG: Ataxia telangiectasia mutated (ATM) signaling network is modulated by a novel poly(ADP-ribose)-dependent pathway in the early response to DNA-damaging agents. J Biol Chem 282: 16441-16453, 2007.
17. Hu Y, Petit SA, Ficarro SB, Toomire KJ, Xie A, Lim E, Cao SA, Park E, Eck MJ, Scully R, *et al*: PARP1-driven poly-ADP-ribosylation regulates BRCA1 function in homologous recombination-mediated DNA repair. Cancer Discov 4: 1430-1447, 2014.

18. Sajish M, Zhou Q, Kishi S, Valdez DM Jr, Kapoor M, Guo M, Lee S, Kim S, Yang XL and Schimmel P: Trp-tRNA synthetase bridges DNA-PKcs to PARP-1 to link IFN-γ and p53 signaling. Nat Chem Biol 8: 547-554, 2012.
19. Tan W, Guan H, Zou LH, Wang Y, Liu XD, Rang WQ, Zhou PK, Pei HD and Zhong CG: Overexpression of TNKS1BP1 in lung cancers and its involvement in homologous recombination pathway of DNA double-strand breaks: Cancer Med 6: 483-493, 2017.
20. Ali SO, Khan FA, Galindo-Campos MA and Yélamos J: Understanding specific functions of PARP-2: New lessons for cancer therapy. Am J Cancer Res 6: 1842-1863, 2016.
21. Spagnolo L, Rivera-Calzada A, Pearl H and Llorca O: Three-dimensional structure of the human DNA-PKcs/Ku70/Ku80 complex assembled on DNA and its implications for DNA DSB repair. Mol Cell 22: 511-519, 2006.
22. Davis AJ, Chen BP and Chen DJ: DNA-PK: A dynamic enzyme in a versatile DSB repair pathway. DNA Repair (Amst) 17: 21-29, 2014.
23. Uematsu N, Weterings E, Yano K, Morotomi-Yano K, Jakob B, Taucher-Scholz G, Mari PO, van Gent DC, Chen BP and Chen DJ: Autophosphorylation of DNA-PKCS regulates its dynamics at DNA double-strand breaks. J Cell Biol 177: 219-229, 2007.
24. Dong J, Zhang T, Ren Y, Wang Z, Ling CC, He F, Li GC, Wang C and Wen B: Inhibiting DNA-PKcs in a non-homologous end-joining pathway in response to DNA double-strand breaks. Oncotarget 8: 22662-22673, 2017.
25. Spagnolo L, Barbeau J, Curtin NJ, Morris EP and Pearl LH: Visualization of a DNA-PK/PARP1 complex. Nucleic Acids Res 40: 4168-4177, 2012.
26. Meek K, Dang V and Lees-Miller SP: DNA-PK: The means to justify the ends? Adv Immunol 99: 33-58, 2008.
27. Povirk LF, Zhou RZ, Ramsden DA, Lees-Miller SP and Valerie K: Phosphorylation in the serine/threonine 2609-2647 cluster promotes but is not essential for DNA-dependent protein kinase-mediated nonhomologous end joining in human whole-cell extracts. Nucleic Acids Res 35: 3869-3878, 2007.
28. Jiang W, Crowe JL, Liu X, Nakajima S, Wang Y, Li C, Lee BJ, Dubois RL, Liu C and Yu X: Differential phosphorylation of DNA-PKcs regulates the interplay between end-processing and end-ligation during nonhomologous end-joining. Mol Cell 58: 172-185, 2015.
29. Wei H and Yu X: Functions of PARylation in DNA damage repair pathways. Genomics Proteomics Bioinformatics 14: 131-139, 2016.
30. Zou LH, Shang ZF, Tan W, Liu XD, Xu QZ, Song M, Wang Y, Guan H, Zhang SM, Yu L, *et al*: TNKS1BP1 functions in DNA double-strand break repair though facilitating DNA-PKcs autophosphorylation dependent on PARP-1. Oncotarget 6: 7011-7022, 2015.
31. Palazzo L, Leidecker O, Prokhorova E, Dauben H, Matic I and Ahel I: Serine is the major residue for ADP-ribosylation upon DNA damage. Elife 7: 34334, 2018.